



A comparison of mercaptothiazoline, mercaptobenzothiazole, mercaptobenzimidazole, and mercaptobenzoxazole as inhibitors of 90/10 cupro-nickel alloy corrosion in seawater  
by Jonathan Paul Storvick

A thesis submitted in partial fulfillment of the requirements for the degree of Doctor of Philosophy in Chemistry  
Montana State University  
© Copyright by Jonathan Paul Storvick (1986)

Abstract:

The corrosion resistance of 90/10 cupro-nickel alloy in seawater is due to the formation of a protective cuprous oxide layer. This corrosion resistance can be improved through the application of inhibitors. The purpose of this investigation was to study the action of 2-mercaptothiazoline (MT), 2-mercaptobenzo-thiazole (MBT), 2-mercaptobenzimidazole (MBI), and 2-mercapto-benzoxazole (MBO) as inhibitors of 90/10 cupro-nickel alloy corrosion in seawater.

A pretreatment procedure was outlined to ensure that experimental results were representative of the alloy and reproducible. Material balance techniques in conjunction with scanning auger microscopy were utilized to study the corrosion processes. A set of base conditions was established and used as a starting point for parameter variation. The individual effects of exposure time, temperature, salinity, and dissolved oxygen were studied to determine a mechanism for the corrosion. During initial exposure the diffusion of OH<sup>-</sup> ions generated by the cathodic reduction of O<sub>2</sub> is likely to be rate limiting. After prolonged exposure the growth rate of oxide is limited by diffusion of cations to the solid-solution interface.

Inhibition of the corrosion was studied with 10<sup>-3</sup> M and 10<sup>-4</sup>M inhibitor concentrations in the seawater. Pretreatment of the surface via immersion in 60°C aqueous solutions of the inhibitors for two minutes was also investigated. The observed order of inhibition efficiency, MBT > MBI = MBO > MT, is explained in terms of a theory of chemisorptive inhibition. Water-insoluble thin polymeric films are formed by a surface reaction between cuprous ions and adsorbed inhibitor molecules via a discharge and nucleation mechanism. The resultant film acts as a barrier to corrosive environments.

A COMPARISON OF MERCAPTOTHIAZOLINE, MERCAPTOBENZOTHAZOLE,  
MERCAPTOBENZIMIDAZOLE, AND MERCAPTOBENZOXAZOLE AS INHIBITORS OF  
90/10 CUPRO-NICKEL ALLOY CORROSION IN SEAWATER

by

Jonathan Paul Storvick

A thesis submitted in partial fulfillment  
of the requirements for the degree

of

Doctor of Philosophy

in

Chemistry

Montana State University  
Bozeman, Montana

May 1986

D 378  
St 755

ii

APPROVAL

of a thesis submitted by

Jonathan Paul Storvick

This thesis has been read by each member of the thesis committee and has been found to be satisfactory regarding content, English usage, format, citations, bibliographic style, and consistency, and is ready for submission to the College of Graduate Studies.

5/16/86  
Date

Gordon Pagenkoff  
Chairperson, Graduate committee

Approved for the Major Department

5/16/86  
Date

Edwin H. Abbott  
Head, Major Department

Approved for the College of Graduate Studies

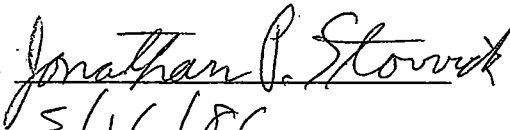
5/28/86  
Date

Henry J. Parsons  
Graduate Dean

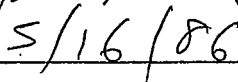
## STATEMENT OF PERMISSION TO USE

In presenting this thesis in partial fulfillment of the requirements for a doctoral degree at Montana State University, I agree that the Library shall make it available to borrowers under rules of the library. I further agree that copying of this thesis is allowable only for scholarly purposes, consistent with "fair use" as prescribed in the U.S. Copyright Law. Requests for extensive copying or reproduction of this thesis should be referred to the University Microfilms International, 300 North Zeeb Road, Ann Arbor, Michigan, 48106, to whom I have granted "the exclusive right to reproduce and distribute copies of the dissertation in and from microfilm and the right to reproduce and distribute by abstract in any format."

Signature



Date



## ACKNOWLEDGMENT

I am very grateful to Dr. Gordon Pagenkopf for his guidance and support throughout the course of my graduate studies. I am also grateful to the faculty of the Chemistry Department and the staff of the CRISS facility for their assistance with this project. Finally, a special thanks to Dave Dobb for his helpful suggestions and ideas, and to all other members of our research group from whom I have learned much.

## TABLE OF CONTENTS

	Page
LIST OF TABLES . . . . .	vii
LIST OF FIGURES. . . . .	viii
ABSTRACT . . . . .	xii
INTRODUCTION . . . . .	1
Copper-Nickel Alloys: Uses, Corrosion Behavior, and Protective Layer Formation . . . . .	1
Auger Spectroscopy . . . . .	8
Material Balance . . . . .	15
Inhibition . . . . .	17
Purpose of Investigation . . . . .	30
EXPERIMENTAL . . . . .	32
Coupon Preparation . . . . .	32
Reactor Design . . . . .	32
Pretreatment of Coupons. . . . .	35
Parameter Measurement and Variation. . . . .	36
Auger Analysis . . . . .	37
Material Balance Derivations . . . . .	46
Inhibitor Experiments. . . . .	56
RESULTS AND DISCUSSION . . . . .	61
PRETREATMENT . . . . .	61
Roughness. . . . .	66
Degreasing . . . . .	69
Acid Pickling. . . . .	70
Sample Storage . . . . .	71
Pretreatment Summary . . . . .	71
MATERIAL BALANCE . . . . .	72
Exposure . . . . .	79
Temperature. . . . .	84
Salinity . . . . .	85
Dissolved Oxygen . . . . .	88
Material Balance Summary . . . . .	89
INHIBITION . . . . .	91
Preliminary Testing. . . . .	92
Spectroscopic Studies. . . . .	95

## TABLE OF CONTENTS (continued)

	Page
Temperature and pH . . . . .	97
Auger Analysis . . . . .	98
Exposure . . . . .	116
Inhibitor Pretreatment . . . . .	119
Inhibition Summary . . . . .	120
CONCLUSIONS. . . . .	124
Pretreatment . . . . .	124
Material Balance . . . . .	124
Inhibition . . . . .	126
REFERENCES CITED . . . . .	130

## LIST OF TABLES

Table	Page
1. Corrosion Inhibitors Reference List . . . . .	23
2. Auger Analysis Conditions . . . . .	39
3. Argon Ion Beam Conditions . . . . .	40
4. Multiplex Data Parameters . . . . .	42
5. Atomic Absorption Conditions for Cu and Ni. . . . .	47
6. Definition of Material Balance Terms. . . . .	49
7. Material Balance Data Set 1 . . . . .	73
8. Material Balance Data Set 2 . . . . .	74
9. Material Balance Data Set 3 . . . . .	75
10. Material Balance Data Set 4 . . . . .	76
11. Material Balance Data Set 5 . . . . .	77
12. Atomic Concentration Percents of Elements on the Surface of Samples Exposed to $10^{-3}$ M MT and $10^{-3}$ M MBT for 48 hours. . . . .	101
13. Inhibitor Efficiencies for 48 Hour Tests at $10^{-4}$ M, $10^{-3}$ M, and Pretreatment. . . . .	118

## LIST OF FIGURES

Figure	Page
1. Critical and Passive Current Densities from Potentiostatic Anodic Polarization Curves for Copper-Nickel Alloys in 1 N H <sub>2</sub> SO <sub>4</sub> , 25°C. . . . .	4
2. Autocatalytic Processes in a Corrosion Pit . . . . .	6
3. Electronic Origin of Auger Electrons . . . . .	10
4. Schematic Diagram of AES Analytical System . . . . .	11
5. Auger General Survey of Coupon Corroded 2 Hours in 1/3 Strength Seawater . . . . .	12
6. Relative Auger Sensitivties of the Elements. . . . .	13
7. Sketch of Electron Flow at Defects in Noble and Sacrificial Coatings . . . . .	19
8. Polarization Curves That Show the Effect of Passivator Concentration on Corrosion. . . . .	25
9. Coupon Dimensions. . . . .	32
10. Stirred Beaker Corrosion Reactor. . . . .	33
11. Tubular Flow Corrosion Reactor. . . . .	35
12. Depth Profile of 1000 Å SiO <sub>2</sub> on Si . . . . .	41
13. Standard Auger Spectra for Nickel . . . . .	43
14. Standard Auger Spectra for Copper . . . . .	44
15. Standard Auger Spectra for Oxygen . . . . .	45
16. Material Balance Flowchart. . . . .	47
17. Resin Column for Recovery of Copper and Nickel. . . . .	48
18. Auger Depth Profile of Coupon Corroded Under Base Conditions. . . . .	52

## LIST OF FIGURES (continued)

Figure	Page
19. Relationship Between $W_o$ and $W_{cp}$ . . . . .	54
20. Structures of MBT, MBI, MBO, and MT . . . . .	57
21. Effects of Surface Roughness on the Corrosion Rate. . . . .	69
22. Dependence of Total Alloy Weight Loss on Exposure. . . . .	80
23. Micrograph of Coupon Corroded Under Base Conditions (1000X). . . . .	81
24. Dependence of Total Alloy Weight Loss on Temperature . . . . .	84
25. Dependence of Total Alloy Weight Loss on Salinity. . . . .	86
26. Dependence of Total Alloy Weight Loss on Dissolved Oxygen. . . . .	89
27. Relation Between Inhibitor Efficiency and Concen- trations for One Hour Stirred Beaker Tests. . . . .	93
28. Dependence of Corrosion Product Weight on Inhi- bitor Concentration . . . . .	94
29. Thiol-Thione Tautomerism of Mercaptobenzothiazole . .	95
30. UV spectra of $5 \times 10^{-5}$ M MBT in 0.1 M $\text{NaSO}_4$ , pH = 3, 6, and 9. . . . .	96
31. Dependence of Total Alloy Weight Loss on Tempera- ture with $10^{-4}$ M MT Inhibition. . . . .	99
32. Dependence of Total Alloy Weight Loss on pH with $10^{-4}$ M MT Inhibition. . . . .	100
33. Depth Profile of Sample Corroded 48 Hours . . . . .	101
34. Auger Survey of Sample Corroded 48 Hours with $10^{-3}$ M MT Inhibition. . . . .	102

## LIST OF FIGURES (continued)

Figure	Page
35. Auger Survey of Sample Corroded 48 Hours with 10 <sup>-3</sup> M MBT Inhibition . . . . .	103
36. Depth Profile of Sample Corroded 48 Hours with 10 <sup>-3</sup> M MT Inhibition . . . . .	104
37. Depth Profile of Sample Corroded 48 Hours with 10 <sup>-3</sup> M MBT Inhibition . . . . .	105
38. Auger Survey of Sample Corroded 48 Hours with 10 <sup>-4</sup> M MBT Inhibition . . . . .	106
39. Depth Profile of Sample Corroded 48 Hours with 10 <sup>-4</sup> M MBT Inhibition . . . . .	107
40. Micrograph of 48 Hour Corroded Coupon (1000X) . . . . .	108
41. Micrograph of Coupon Corroded 48 Hours with 10 <sup>-3</sup> M MT Present (1000X) . . . . .	109
42. Micrograph of Coupon Corroded 48 Hours with 10 <sup>-4</sup> M MT Present (1000X) . . . . .	110
43. Micrograph of Coupon Corroded 48 Hours with 10 <sup>-4</sup> M MT Present (10,000X) . . . . .	111
44. Micrograph of Coupon Corroded 48 Hours with 10 <sup>-4</sup> M MBT Present (1000X) . . . . .	112
45. Micrograph of Coupon Corroded 48 Hours with 10 <sup>-4</sup> M MBI Present (1000X) . . . . .	113
46. Micrograph of Coupon Corroded 48 Hours with 10 <sup>-4</sup> M MBI Present (2000X) . . . . .	113
47. Micrograph of Coupon Corroded 48 Hours with 10 <sup>-4</sup> M MBO Present (1000X) . . . . .	114
48. Structure of the Surface Film on 90/10 Cupro- Nickel Alloy Formed with 10 <sup>-4</sup> M Inhibitors Present in Seawater . . . . .	116
49. Dependence of Tarnish Rate on Exposure with 10 <sup>-4</sup> M Inhibitors Present. . . . .	117

## LIST OF FIGURES (continued)

Figure	Page
50. Dependence of Tarnish Rate on Exposure with $10^{-3}$ M Inhibitors Present . . . . .	119
51. Dependence of Tarnish Rate on Exposure with Inhibitors Pretreated on the Surface . . . . .	121
52. Proposed Polymeric Structure of Cu(I)MBT . . . . .	128

## ABSTRACT

The corrosion resistance of 90/10 cupro-nickel alloy in seawater is due to the formation of a protective cuprous oxide layer. This corrosion resistance can be improved through the application of inhibitors. The purpose of this investigation was to study the action of 2-mercaptothiazoline (MT), 2-mercaptobenzothiazole (MBT), 2-mercaptobenzimidazole (MBI), and 2-mercaptobenzoxazole (MBO) as inhibitors of 90/10 cupro-nickel alloy corrosion in seawater.

A pretreatment procedure was outlined to ensure that experimental results were representative of the alloy and reproducible. Material balance techniques in conjunction with scanning auger microscopy were utilized to study the corrosion processes. A set of base conditions was established and used as a starting point for parameter variation. The individual effects of exposure time, temperature, salinity, and dissolved oxygen were studied to determine a mechanism for the corrosion. During initial exposure the diffusion of  $\text{OH}^-$  ions generated by the cathodic reduction of  $\text{O}_2$  is likely to be rate limiting. After prolonged exposure the growth rate of oxide is limited by diffusion of cations to the solid-solution interface.

Inhibition of the corrosion was studied with  $10^{-3}$  M and  $10^{-4}$  M inhibitor concentrations in the seawater. Pretreatment of the surface via immersion in  $60^\circ\text{C}$  aqueous solutions of the inhibitors for two minutes was also investigated. The observed order of inhibition efficiency,  $\text{MBT} > \text{MBI} \approx \text{MBO} > \text{MT}$ , is explained in terms of a theory of chemisorptive inhibition. Water-insoluble thin polymeric films are formed by a surface reaction between cuprous ions and adsorbed inhibitor molecules via a discharge and nucleation mechanism. The resultant film acts as a barrier to corrosive environments.

## INTRODUCTION

## Copper-Nickel Alloys: Uses, Corrosion Behavior, and Protective Layer Formation

The cost of corrosion and protection against corrosion in the United States has been estimated at eight billion dollars per year<sup>1</sup>. Although this is a very large cost, it is not surprising when considering corrosion occurs whenever metals and other materials are used. Corrosion is inevitable, but in many cases its cost can be reduced, and catastrophic failure may be prevented.

Corrosion may be defined as the destruction or deterioration of a material due to its reaction with the environment other than by mechanical means. This study is concerned with the oxidation of 90/10 cupro-nickel alloy due to exposure to seawater.

Copper and copper alloys are employed extensively for fresh water and marine applications. The main reasons for these uses include (a) excellent corrosion and biofouling resistance, (b) good mechanical workability, (c) galvanic compatibility with other copper alloy system components, (d) reliability and economy. Applications for copper alloys include condenser tubing, ocean thermal energy conversion heat exchangers, and piping systems for offshore seawater platforms<sup>2,3</sup>.

A problem commonly encountered in conjunction with corrosion is fouling. Two major problems associated with fouling are lowered heat transfer capability and inhibited flow of liquids through

pipes. The best way to prevent fouling is to choose an alloy which is resistant, like cupro-nickel alloys. Fouling resistance is primarily due to release of cupric ions during corrosion. These cupric ions are toxic to marine organisms attaching to the metal surface<sup>4</sup>. Although resistant organisms may colonize, a buildup of non-protective corrosion products such as paratacamite ( $\text{Cu}_2(\text{OH})_3\text{Cl}$ ) between the organisms and the metal surface will allow the organisms to be swept away<sup>5</sup>.

The long-term, steady-state corrosion rate of 90/10 cupro-nickel has been shown to be less than 0.5 mils per year<sup>3</sup>. One result of the excellent corrosion and fouling resistance is a reduction in the required pipe thickness and diameter for many applications.

Corrosion resistance of copper alloys is primarily due to the formation of a surface oxide film acting as a barrier between the metal and the environment. Copper dissolves anodically in aqueous environments forming the divalent  $\text{Cu}^{2+}$ . The equilibrium relation



is displaced far to the right ( $K = 1.7 \times 10^6$ ). However, if complexes are formed, as between  $\text{Cu}^+$  and  $\text{Cl}^-$  in a chloride solution, the depletion of  $\text{Cu}^+$  to  $\text{CuCl}_2^-$  favors  $\text{Cu}^+$  as the major dissolution product. Hence the oxide film formed is principally composed of  $\text{Cu}_2\text{O}$ .<sup>6</sup> The film may also contain alloying metals in the oxide lattice, giving the film its corrosion resistant properties.

Cupro-nickel alloys are resistant to corrosion in many applications, due to doping of the  $\text{Cu}_2\text{O}$  lattice with  $\text{Ni}^{2+}$  ions.

This doping lowers the electrical and ionic conductivity of the protective film, rendering it more inert to electrochemical activity.

Other metals are added to the alloy to improve mechanical properties and/or to increase corrosion resistance. Iron is added to enhance corrosion resistance in seawater. The lowest corrosion rates without iron additions are at the 25 at 30% nickel level, whereas with iron these rates are achieved at a 10% nickel level<sup>7</sup>. The effect is an enhancement of nickel incorporation into the  $\text{Cu}_2\text{O}$  lattice. The metal reactivity is related to chemisorbed oxygen films, which are favored by electron vacancies in the metal. These adsorbed oxygen films are not diffusion barriers, but act instead to decrease metal reaction kinetics by impeding metal ion hydration. Thus alloyed transition metals (Fe, Mn) added in small amounts, shift the critical Ni composition for passivity to lower values, as shown in Figure 1. This is explained by the electron configuration theory of passivity<sup>8</sup>.

Fontana and Greene<sup>1</sup> classify corrosion by the forms in which it is displayed, based on the appearance of the corroded metal. These forms are described as (1) uniform, or general attack, (2) galvanic, or two-metal corrosion, (3) crevice corrosion, (4) pitting, (5) intergranular corrosion, (6) selective leaching, or parting, (7) erosion corrosion, and (8) stress corrosion. In most applications the primary reason for failure is localized rather than general attack, so uniform corrosion is not a problem. Copper-nickel alloy systems are galvanically compatible with other

copper alloy system components such as pumps and valves, so two-metal corrosion is generally not a problem either.

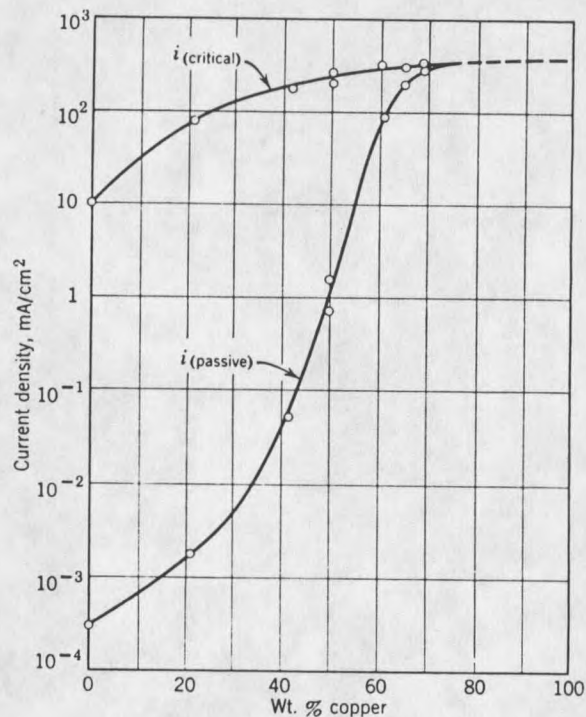


Figure 1. Critical and Passive Current Densities from Potentiostatic Anodic Polarization Curves for Copper-Nickel Alloys in 1 N H<sub>2</sub>SO<sub>4</sub>, 25°C.<sup>8</sup>

Crevice corrosion is usually associated with small volumes of stagnant solution in protected areas such as holes, crevices, gasket surfaces, lap joints, or under surface deposits. The crevice corrosion area must be wide enough to permit liquid entry, but small enough to maintain a stagnant zone. During the initial stages of corrosion the oxygen in the zone is depleted, while the surrounding metal has an adequate supply, thus the depleted region becomes anodic and corrodes more rapidly. Metal dissolution in the crevice produces cations which must be balanced by migration

of chloride ions into the crevice. The formation of soluble metal chlorides increases the metal dissolution rate, and through migration the result is a rapidly accelerating or auto-catalytic process.

Pitting is a form of extremely localized attack with holes in the metal as the end result. It is an autocatalytic process, whereby corrosion reactions within a pit produce conditions which stimulate continued growth. This process is shown in Figure 2. It is very similar to crevice corrosion in that the formation of soluble metal chlorides increases the metal dissolution rate, and an anodic current develops. Adjacent areas become cathodic resulting in the formation of an active-passive cell.

Copper-nickel alloys are not susceptible to intergranular corrosion, and selective leaching or dealloying is not a problem either as long as temperatures are kept low (<100°C).<sup>2</sup> Copper-zinc alloys do suffer from dealloying, however. The process is referred to as dezincification.

Erosion corrosion is an acceleration in the rate of deterioration due to the relative movement between a corrosive fluid and the metal surface. At high flow rates shear forces can strip off protective  $\text{Cu}_2\text{O}$  layers and cause erosion corrosion or impingement damage. The more adherent and protective the passive film on an alloy, the greater its resistance will be to impingement or erosion corrosion. Copper-nickel alloys exhibit excellent corrosion resistance at low velocities, but are subject to erosion

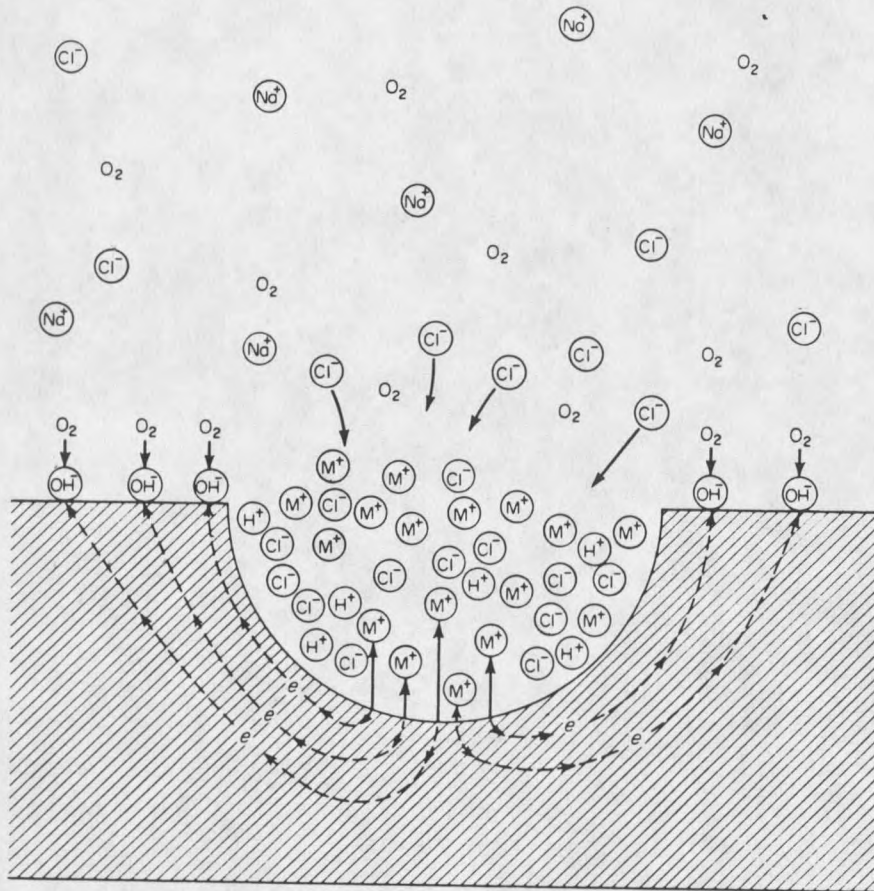


Figure 2. Autocatalytic Processes in a Corrosion Pit<sup>1</sup>.

corrosion at higher flow rates. Other factors which affect erosion corrosion include pH, water temperature, oxygen content, gas bubbles, and silt particles in the corrosive medium<sup>9</sup>.

Stress corrosion cracking occurs when a metal is placed in tensile stress in a corrosive environment. Important variables which affect this type of corrosion are temperature, solution composition, metal composition, stress, and metal structure. From outward appearance one might conclude brittle mechanical fracture was occurring, while local corrosion processes are actually

responsible. These cracks may form intergranularly or transgranularly, the most susceptible copper alloys are the brasses when exposed to ammonia or amines in the presence of oxygen and moisture<sup>8</sup>. Cupro-nickel alloys in condenser applications do not generally suffer stress corrosion cracking, as stresses are low and environmental conditions for cracking are not present.

The eight forms of corrosion have varying degrees of importance in the corrosion of cupro-nickel alloys in seawater. Some play an important role and some do not. Certain aggressive ions and molecules such as  $\text{Cl}^-$ ,  $\text{S}^{2-}$  and  $\text{NH}_3$  can be important in promoting corrosion of cupro-nickel alloys.

Chloride forms complex ions of the form  $\text{CuCl}_x^{1-x}$  with cuprous ions and may accelerate metal loss. The mechanism has been described as follows:



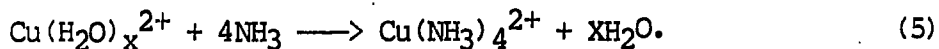
The kinetics are primarily governed by diffusion of cuprous complexes from the surface, the final step in this case is rate determining<sup>10-13</sup>.

Copper-nickel alloys suffer accelerated corrosion in sulfide polluted seawater. The presence of dissolved sulfide interferes with the formation of a passive layer, as a porous cuprous sulfide film forms rather than a protective cuprous oxide layer. When oxygen is present the process is accelerated even further. The ionic and electrical conductivity is increased by  $\text{S}^{2-}$  ions

incorporated into the oxide lattice, leading to lowered resistance to anodic reactions<sup>14,15</sup>.

Sulfide is present in seawater as a result of decay in marine organisms and plants. The oxidation of organic material can lead to depletion of oxygen. Under these anaerobic conditions sulfate reducing bacteria can reduce sulfates to sulfides, thus increasing the corrosion rates.

Ammonia has been shown to attack copper and copper alloys, resulting in the formation of a soluble copper ammonia complex. The reaction of hydrated copper ions with ammonia is as follows:



Copper and its alloys are well suited for handling anhydrous ammonia solutions, but with water present this is not the case<sup>2</sup>.

The corrosion product layer which forms when copper-nickel alloys corrode is  $\text{Cu}_2\text{O}$ , and is protective of the alloy against further corrosion. Although the  $\text{Cu}_2\text{O}$  is a "passive" oxide it is not completely unreactive, and chloride ions in seawater continue to dissolve the oxide while new  $\text{Cu}_2\text{O}$  is formed at the metal surface. The  $\text{Cu}_2\text{O}$  reaches a protective thickness only after several days of exposure, and grows by a solid-state mechanism involving migration of cations through the oxide layer to react with adsorbed anions on the surface.

#### Auger Spectroscopy

Auger Emission Spectroscopy (AES) was utilized in this study for analysis of corrosion products formed on the surface of the

alloy. This surface analytical technique provides several types of information including elemental concentrations, depth profiles, and scanning electron micrographs showing surface morphology. It is a truly surface analytical technique as the auger electrons detected usually originate within a surface volume  $\sim 30\text{\AA}$  deep<sup>16</sup>.

Surface analytical techniques such as Auger spectroscopy (AES), Electron Spectroscopy for Chemical Analysis (ESCA) or (XPS), and Secondary Ion Mass Spectroscopy (SIMS) have recently become popular in corrosion studies<sup>17-22</sup>. ESCA provides chemical state information while AES yields detailed chemical analysis with depth through ion milling. SIMS is a very sensitive technique for a number of elements; the sensitivity for one particular element depends very much on the composition of the sample however. Chemical information is also obtainable with SIMS. Auger Spectroscopy was selected for this study as quantitative analysis with depth was desired.

The AES technique for chemical analysis is based on the Auger radiationless process, shown in Figure 3. When a core level of a surface atom is ionized by the electron beam (1-10 KeV), the atom decays through an electronic rearrangement leaving the atom doubly ionized. The energy difference between the two states is imparted to the ejected auger electron, whose kinetic energy is characteristic of the parent atom. If the auger process occurs within several angstroms of the surface, the auger electrons may escape without loss of energy, giving rise to peaks in the secondary electron distribution. As there is a very large



























































































































































































































































